Supplementary Materials for "Stochastic processes drive rapid genomic divergence during experimental range expansions"

Christopher Weiss-Lehman[1,2], Silas Tittes[1], Nolan C. Kane[1], Ruth A. Hufbauer[3,4], Brett A. Melbourne*[,1]

1: Department of Ecology and Evolutionary Biology, University of Colorado, Boulder, CO, 80309.

2: Current affiliation: Department of Ecology, Evolution, and Behavior, University of Minnesota, Saint Paul, MN 55108

3: Department of Bioagricultural Sciences and Pest Management and Graduate Degree Program in Ecology, Colorado State University, Fort Collins, CO 80523-1177.

4: UMR Centre de Biologie et Gestion des Populations, INRA, 34988 Montferrier sur Lez, France

Published in *Proceedings of the Royal Society: B* (DOI: 10.1098/rspb.2019.0231)

Supplementary file descriptions

QualTable.csv

This table contains information on the number of reads and average quality scores before and after filtering for all experimental populations. Populations are identified by replicate number, generation, treatment (structured or shuffled), and location (core, edge, or NA).

AccessionTable.txt

This table contains the NCBI Sequence Read Archive accession numbers for all experimental populations. Populations are identified by replicate, generation, and location separated by underscores.

Supplementary methods

Assessing the role of selection on mutations and rare alleles

The variable patterns of changes in genomic diversity observed in our data, while likely caused by neutral processes, could be generated by selection acting on *de novo* mutations arising in individual replicates or on rare alleles from the source population only sampled by a small number of landscapes. To test for the first possibility, we identified putatively *de novo* mutations in our data as alleles not sampled in any of the founding populations (as samples from the source population) and present in only a single eighth-generation landscape. We quantified single nucleotide polymorphism (SNP) frequencies using Popoolation2 [47], restricting the set of potential *de novo* mutations to those with coverage between 4 and 22 based on the distribution of average depths across populations (Figs. S1 and S2) and with a minimum minor allele count of 4 to avoid including potential sequencing errors. We further used the Ensembl Metazoa (release 41) web interface for the Variant Effect Predictor software [48, 49] to identify in which region of the genome each *de novo* mutation occurred, and to predict what consequences the mutations could have for protein coding genes, if any. While this process represents a rigorous threshold for identifying *de novo* mutations, the possibility exists that some alleles identified as *de novo* mutations were in fact rare variants missed in the pooling and sequencing of the founding populations. To assess this possibility, we also performed a mechanistic detection simulation based on experimental parameters to calculate the probability of identifying an allele in the source population as a function of its frequency. We call this the *detection model*.

As our criteria for identifying *de novo* mutations included that they be absent from all of the founding populations, for the detection model we conducted simulations replicating the experimental design and sampling processes used to evaluate our ability to detect rare alleles in

the founding populations. Mirroring our statistical analysis, we only considered bi-allelic sites and explored a gradient of minor allele frequencies in the source population, ranging from 5 x 10^{-5} to 0.01. We began each simulation by using the minor allele frequency to generate 40 alleles for each of the 37 founding populations, simulating the initial sampling of founders from the source population. We then simulated pooling by sampling the founder alleles with replacement and according to the empirical distribution of sampling depths from the founder pools (Fig. S2). We further required the counts to fall between 4 and 22, matching the cutoffs used in the empirical analyses. Using these simulated allele counts, we quantified the probability of detecting the minor allele as the proportion of times it was absent in all 37 simulated founding populations. We repeated this analysis 10,000 times for 50 different minor allele frequencies ranging from 5 x 10^{-5} to 0.01. We calculated the mean detection probability with high precision for each minor allele frequency (Fig. S6). This process likely underestimates the true detection probability since it does not include the populations from the eighth generation that provide further samples to detect standing variation (i.e. we also required *de novo* mutations not be present in more than one eighth-generation landscape). Thus, these simulations indicate we should be able to reliably distinguish between new mutations and even exceedingly rare standing variation.

Using the *de novo* mutations identified by our criteria, we then created a new data set for the changes in nucleotide diversity, $\Delta\pi$, associated with windows containing a putative *de novo* mutation. As we defined *de novo* mutations as those arising in only a single landscape, the datum associated with each mutation represents the change in diversity at a genomic window within a single population, rather than the mean across replicates as was used to calculate $\overline{\Delta\pi}$. In this way, reductions in nucleotide diversity attributable to the *de novo* mutations could be directly

assessed. Changes in nucleotide diversity from the founders to the 8th generation were calculated as before. If a mutation occurred within 2,000 bp of the edge of a window, the average nucleotide diversity of the two windows (original and nearest adjacent window to the mutation) was used to compute the change in diversity associated with that mutation. We analyzed these data with a linear model identical to the model used to assess genome wide changes in nucleotide diversity. If selection on these alleles were driving increased variability in genomic changes among replicates, the windows containing them should demonstrate reduced nucleotide diversity as a result.

To address the second possible mechanism by which selection could lead to variable genomic changes among replicates, namely selection acting on rare alleles only sampled by some of the founder populations, we constructed a model to evaluate the probability of rare alleles being sampled by only a subset of landscapes which we call the *sampling model*. Assuming allele frequencies in the original source population are at Hardy-Weinberg equilibrium [50], the frequency of individuals with at least one copy of an allele at frequency p is given by

$$\alpha = 2p(1\text{-}p) + p^2 \qquad (1).$$

Then, assuming random sampling of the source population to form the founding populations for each replicate, as was done experimentally, the probability of a single founding population not sampling the allele is $(1 - \alpha)^{20}$ as each population consisted of 20 beetles. The probability of k populations simultaneously not sampling the allele is thus given by

$$\phi = (1 - \alpha)^{20k} \qquad (2).$$

We examined the probability ϕ as a function of both the initial allele frequency (p) and the number of founding populations to not sample the allele (k).

Supplementary results

Assessing the role of selection on mutations and rare alleles

We identified 66 putatively *de novo* mutations in our data. While some of these alleles may in fact represent rare, unidentified variants from the source population, analysis of models evaluating the probability of detecting rare alleles in our data (*detection model*) and the probability of rare alleles in the source population being sampled in only a subset of founding landscapes (*sampling model*) indicates this is unlikely for two reasons. First, even if an allele is at a frequency as low as 0.002 in the source population, the detection model estimates a 0.5 probability of identifying the allele in at least one of the founding populations. This probability increases rapidly to over 0.95 for alleles at frequencies of 0.008 or more in the source population (Fig. S6). Second, as our criteria for a *de novo* mutation requires the allele to be present in only one of the eighth-generation populations, for it to result from a rare variant in the source population, that rare variant would be sampled in few founding populations and by definition be lost in all but one of them. If the rare variant were at a frequency of 0.008 in the source population, the sampling model suggests the probability of only 5 or fewer founding populations sampling the allele is 0.004 or lower (Fig. S5). Thus, the 66 alleles identified as *de novo* mutations are unlikely to include rare alleles present but unidentified in the source population.

We detected an average of 2 *de novo* mutations that arose and persisted in each landscape, but there was substantial variation around this with 8 landscapes containing none and 1 landscape with 8 *de novo* mutations. Only 6 of the 66 alleles were detected in both the core and edge populations from the same landscape, suggesting relatively little gene flow between core and edge populations in most landscapes. Changes in nucleotide diversity for windows associated with *de novo* mutations were close to zero, revealing no significant increases or

decreases in nucleotide diversity for core, edge, or shuffled populations (Fig. S4; all confidence intervals overlap 0). Additionally, there was no significant difference in the change in nucleotide diversity between edge populations and core or shuffled populations (likelihood ratio test for the effect of spatial structure: $p = 0.21$). The small change in nucleotide diversity, comparable to changes seen for core and shuffled populations, suggests that while some mutations arose during expansion, selection upon them was not an important factor in causing the large, widespread, and variable reductions in diversity observed in edge populations.

Supplementary Literature Cited

47. Kofler R, Pandey RV, Schlotterer C. 2011 PoPoolation2: identifying differentiation between populations using sequencing of pooled DNA samples (Pool-Seq). *Bioinformatics* **27**, 3435–3436.

48. McLaren W *et al*. 2010 Deriving the consequences of genomic variants with the Ensembl API and SNP Effect Predictor. *Bioinformatics* **26**, 2069-2070.

49. McLaren W *et al*. 2016 The ensembl variant effect predictor. *Genome biology* **17**, 122.

50. Stern C. 1943 The Hardy-Weinberg law. *Science* **97**, 137-138.

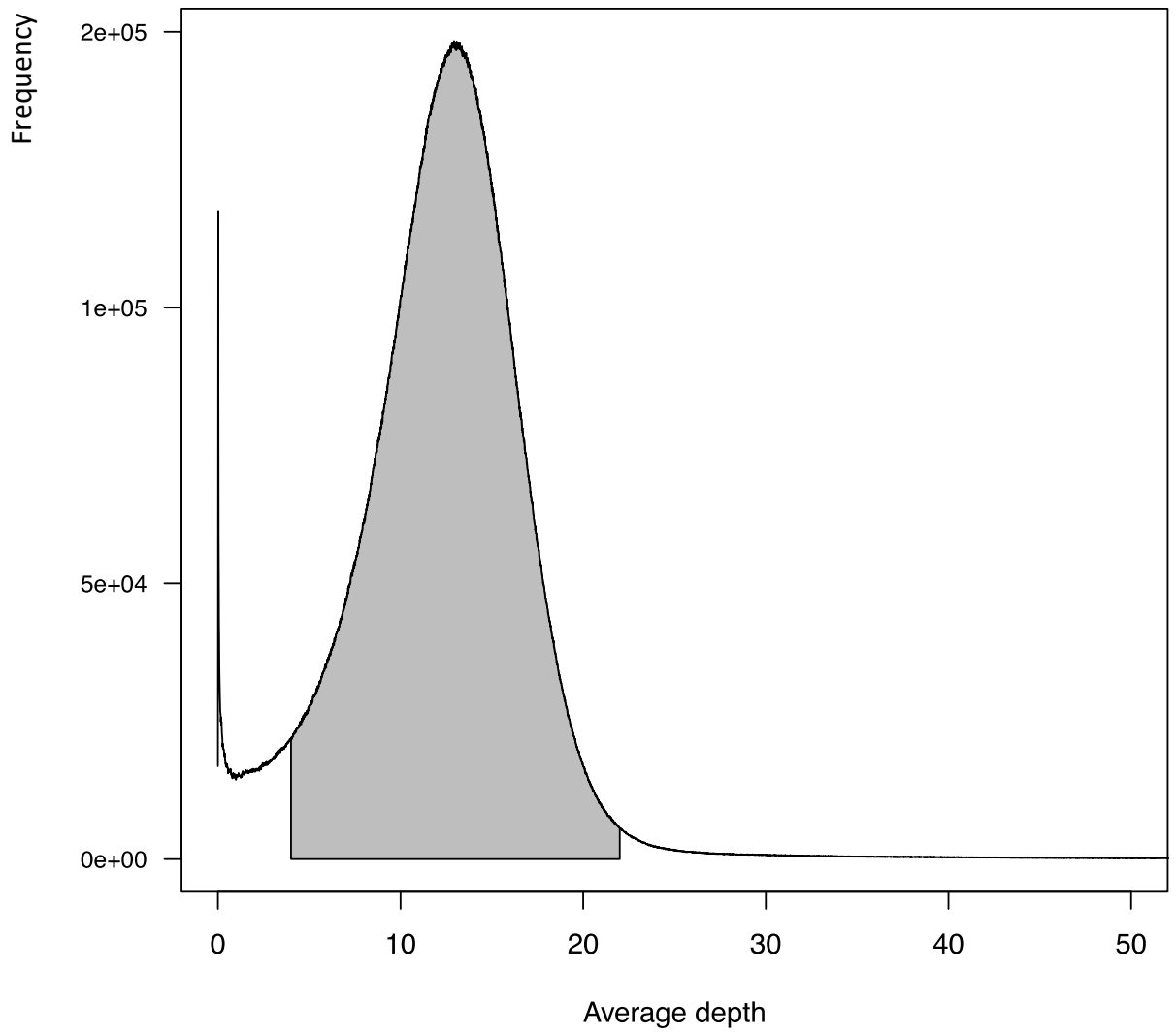

Figure S1: Average depth profile of the aligned sequencing reads. The shaded grey region corresponds to the depth cutoffs used in our analyses (4 and 22).

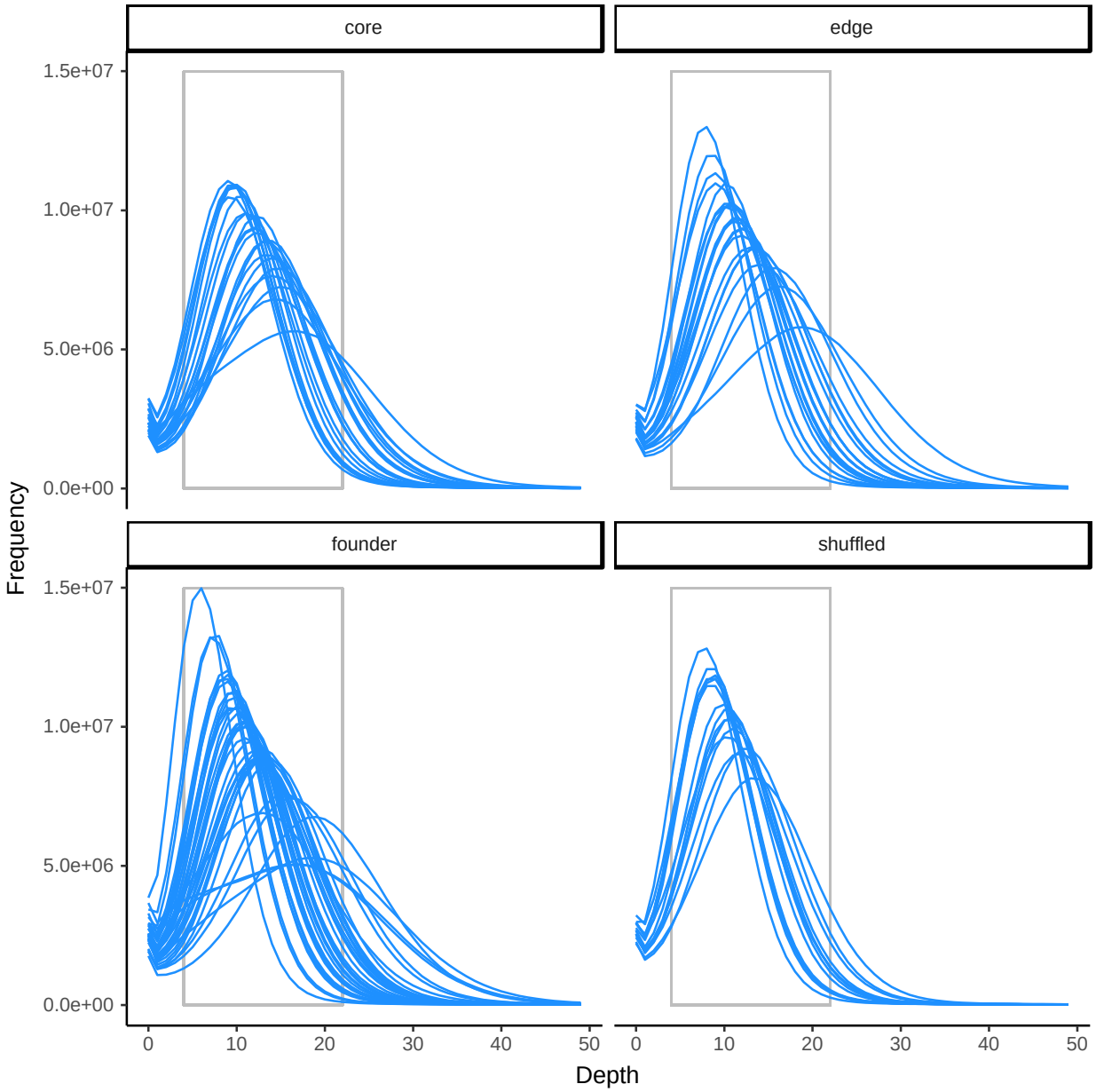

Figure S2: Depth profiles of aligned sequencing reads in individual populations. Each line corresponds to a single population with populations grouped according to the experimental design. The shaded grey region corresponds to the depth cut offs used in our analysis (4 and 22).

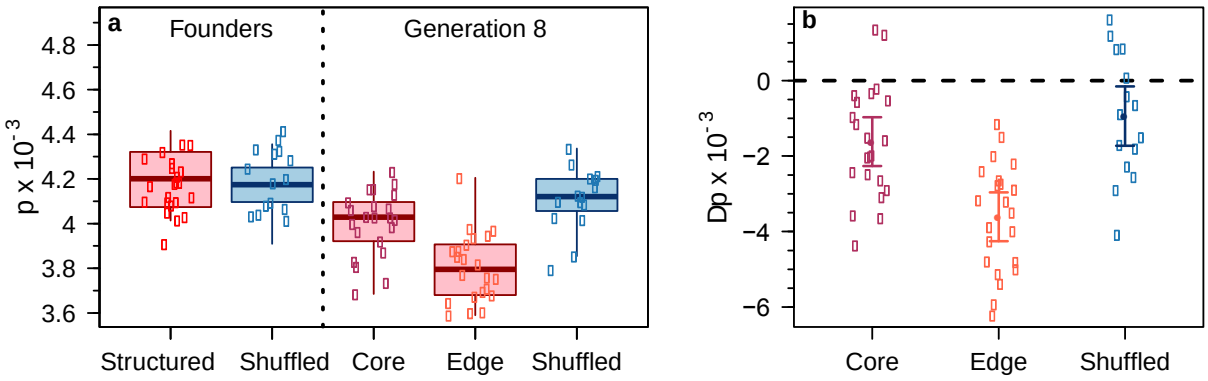

Figure S3: Nucleotide diversity contained in the X chromosomes of founding and generation eight populations. Mean nucleotide diversity (π) across the X chromosome for all experimental populations is shown in (a). The derived data (mean π across windows) are plotted as individual points and distributions among replicates are shown with standard Tukey box plots. Differences from founders to generation eight populations of the same landscapes are shown in (b). Differences were calculated as the generation 8 value minus the founding population from the same landscape, so a negative value indicates a loss of diversity. No change is indicated by a horizontal dashed line at 0. Derived data are shown as points and model estimated means and 95% confidence intervals are shown by the solid points and error bars. Like the autosomal results, edge populations show significantly greater reductions in diversity from the founders compared to core and shuffled populations (likelihood ratio test for effect of spatial structure: $p < 0.001$). Sample sizes are 22 for structured landscapes (encompassing the structured founders and core and edge populations from generation 8) and 15 for both generations of shuffled landscapes.

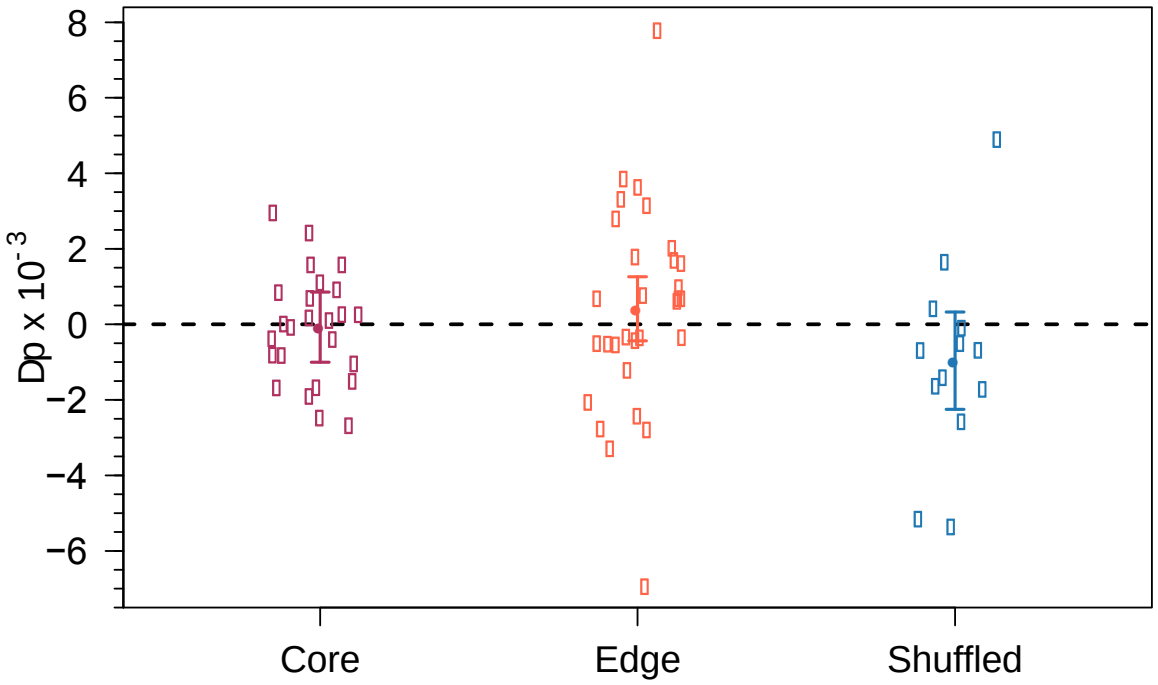

Figure S4: Change in nucleotide diversity for windows with identified *de novo* mutations. The change in nucleotide diversity for each window was calculated as the value for the window in the generation eight population minus the value for the same window in the founding population from the same landscape, so negative values indicate loss of nucleotide diversity. The dashed, horizontal line at 0 indicates no change. Results are shown for *de novo* mutations identified in core populations (n = 28), edge populations (n = 31), and shuffled populations (n = 13) from the eighth generation as indicated on the figure. Data for individual windows associated with identified *de novo* mutations are shown as hollow points and model estimated means and 95% confidence intervals are shown as solid points and error bars. The changes in nucleotide diversity for windows containing *de novo* mutations were not significantly different from 0 for any population group and were similar across groups (likelihood ratio test: p = 0.21), indicating *de*

novo mutations were not responsible for the consistent, widespread changes to nucleotide diversity arising during range expansion.

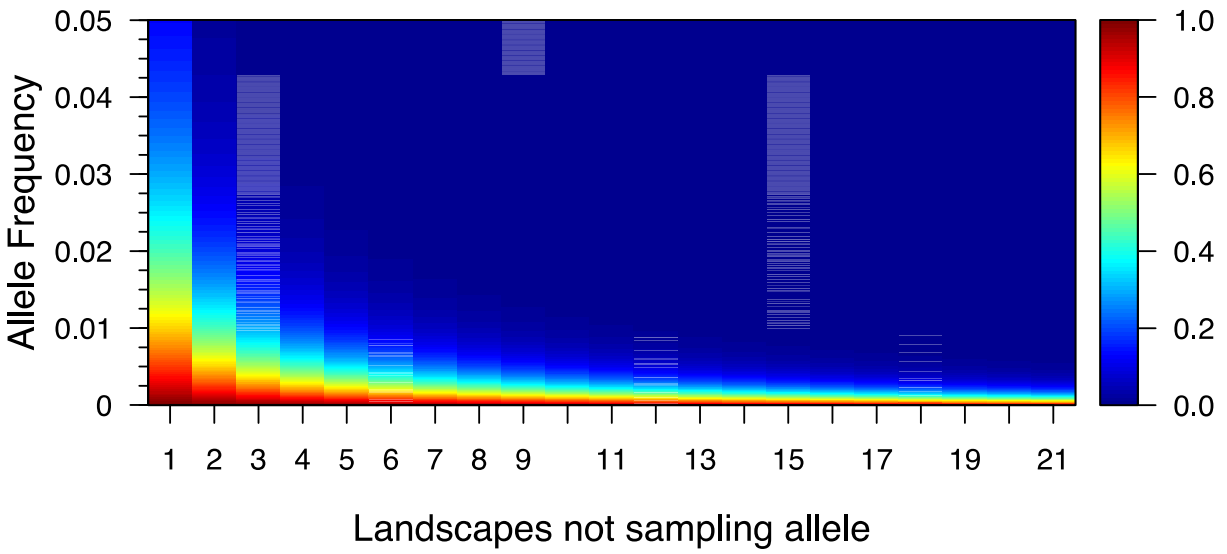

Figure S5: Probability of a given number of founding structured populations failing to sample an allele present in the source population at relatively low frequencies according to the sampling model. Probabilities are calculated assuming Hardy-Weinberg equilibrium in the source population and random sampling as described in the supplemental text. Probability is indicated via color according to the color key to the right of the figure while allele frequency in the source population and the number of landscapes failing to sample vary along the axes as indicated on the figure. The results indicate a quite low probability of more than a small handful of landscapes failing to sample an allele from the source population at even relatively low frequencies.

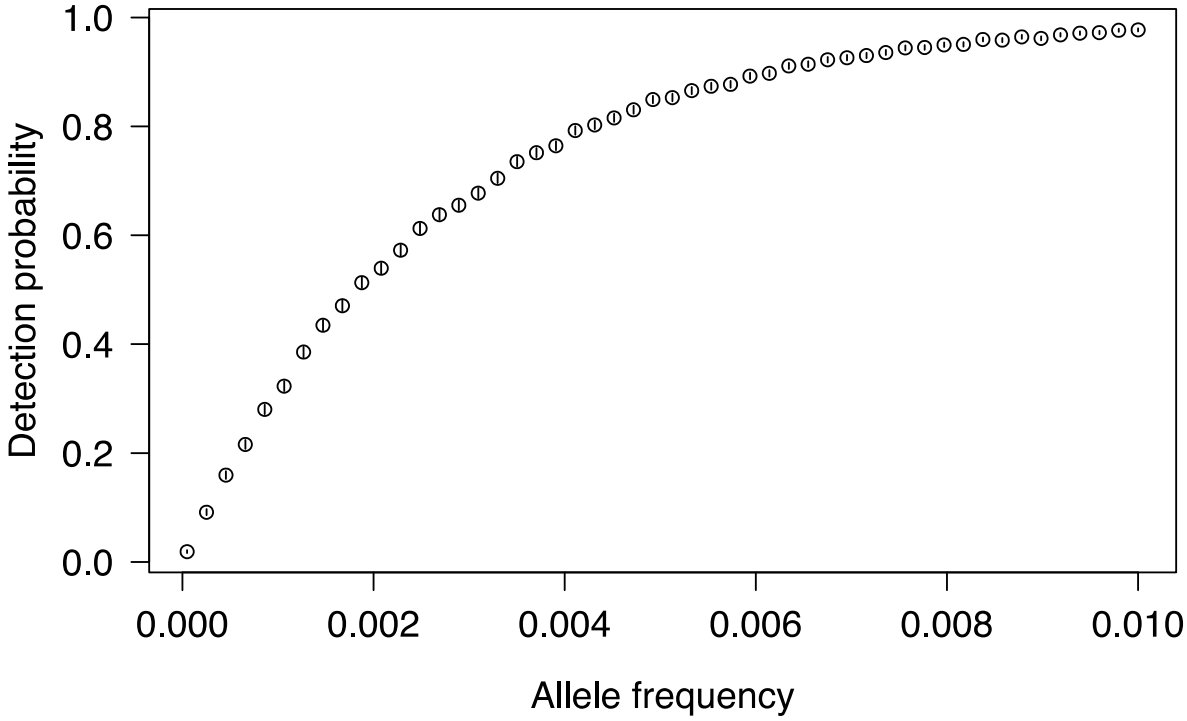

Figure S6: Results of the detection model evaluating our ability to detect rare alleles from the source population in the founders. Each point is the average detection probability of 10,000 simulations and the error bars are 95% confidence intervals. The rapid increase of detection probability with allele frequency indicates we are able to identify most *de novo* mutations with a high degree of accuracy.